Received: 3 February 2018 | Accepted: 5 July 2018

DOI: 10.1002/jcp.27132

ORIGINAL RESEARCH ARTICLE

WILEY Journal of Cellular Physiology

Caspase-1-dependent mechanism mediating the harmful impacts of the quorum-sensing molecule N-(3-oxo-dodecanoyl)-L-homoserine lactone on the intestinal cells

Shiyu Tao | Qinwei Sun | Liuping Cai | Yali Geng | Canfeng Hua | Yingdong Ni | Ruqian Zhao

Key Laboratory of Animal Physiology & Biochemistry, Ministry of Agriculture, Nanjing Agricultural University, Nanjing, Jiangsu, China

Correspondence
Dr. Yingdong Ni, Key Laboratory of Animal Physiology & Biochemistry, Nanjing Agricultural University, Nanjing 210095, China.
Email: niyingdong@njau.edu.cn

Funding information
National Nature Science Foundation of China, Grant/Award Number: 31572433; National Basic Research Program of China, Grant/Award Number: 2011CB100802; Program for New Century Excellent Talents in University, Grant/Award Number: NCET-13–0862; Priority Academic Program Development of Jiangsu Higher Education Institutions

Abstract

N-(3-oxododecanoyl)-L-homoserine lactone (3-oxo-C12-HSL), a quorum-sensing (QS) molecule produced by Gram-negative bacteria in the gastrointestinal tract, adversly impacts host cells. Our previous study demonstrated that 3-oxo-C12-HSL induced a decrease in cell viability via cell apoptosis and eventually disrupted mucin synthesis from LS174T goblet cells. However, the molecular mechanism underlying cell apoptosis and whether pyroptosis was involved in this process are still unknown. In this study, we emphasized on the caspases signal pathway and sterile inflammation to reveal the harmful effects of 3-oxo-C12-HSL on LS174T goblet cells. Our data showed that 3-oxo-C12-HSL is a major inducer of oxidative stress indicated by a high level of intracellular reactive oxygen species (ROS). However, TQ416, an inhibitor of paraoxonase 2, can effectively block oxidative stress. A higher ROS level is the trigger for activating the caspase-1 and 3 cascade signal pathways. Blockade of ROS synthesis and caspase-1 and 3 cascades can obviously rescue the viability of LS174T cells after 3-oxo-C12-HSL treatment. We also found that paralleled with a higher level of ROS and caspases activation, an abnormal expression of proinflammatory cytokines was induced by 3-oxo-C12-HSL treatment; however, the blockage of TLRs-NF-κB pathway cannot restore cell viability and secretary function. These data collectively indicate that 3-oxo-C12-HSL exposure induces damages to cell viability and secretary function of LS174T goblet cells, which is mediated by oxidative stress, cell apoptosis, and sterile inflammation. Overall, the data in this study will provide a better understanding of the harmful impacts of some QS molecules on host cells and their underlying mechanism.

KEYWORDS
3-oxo-C12-HSL, apoptosis, innate immune, LS174T goblet cells, oxidative stress

1 | INTRODUCTION

Intestinal mucosal surfaces serve as the first line of defense against various bacterial and viral infections between the epithelium and the

Abbreviations: 3-oxo-C12-HSL, N-(3-oxododecanoyl)-L-homoserine lactone; MDA, Malondialdehyde; Muc 2, Mucin 2; NAC, N-acetyl-L-cysteine; PAMP, Pathogen-associated molecular patterns; PAS, Periodic acid-schiff; PON2, Paraoxonase 2; PRR, Pattern recognition receptors; QS, Quorum-sensing; ROS, Reactive oxygen species; TLRs, Toll like receptors; TQ416, Triazolo[4,3-a] quinolone.

luminal content (Ivanov & Honda, 2012; Johansson, Sjövall, & Hansson, 2013; Kim & Ho, 2010). Mucins, one kind of glycoproteins, are synthesized and secreted by goblet cells, which play a vital role as a physiological barrier via mucus layer formation (Linden, Sutton, Karlsson, Korolik, & McGuckin, 2008). Impairment of the mucus layer leads to the invasion of pathogenic microorganisms and then threats the ecosystem's balance of the gut as well as the homeostasis of the host immune responses (Parlato & Yeretssian, 2014). It is well documented that abnormalities in mucin's expression make gastrointestinal epithelium more susceptible to infections by pathogenic bacteria, eventually resulting in several diseases, such as severe colitis and intestinal hyper-permeability (Johansson et al., 2014; Shan et al., 2013; Van der Sluis et al., 2006).

Quorum sensing (QS) regulate bacteria behaviors at the population level by an intercellular signaling mechanism (Schuster & Greenberg, 2006). Numerous Gram-negative bacteria use these small lipid-soluble and membrane-permeable molecules as the autoinducer of QS to trigger the innate immune response and induce cells apoptosis in host cells (Li, Hooi, Chhabra, Pritchard, & Shaw, 2004; Schwarzer et al., 2012; Shiner, Rumbaugh, & Williams, 2005; Smith et al., 2001; Valentine, Anderson, Papa, & Haggie, 2013). As a QS molecule, N-(3-oxododecanoyl)-homoserine lactone (3-oxo-C12-HSL) produced by Gram-negative bacteria in the gut can perturb epithelial integrity, enhance epithelial permeability, and lead to the development of intestinal diseases (Eum, Jaraki, Bertrand, András, & Toborek, 2014). The major characteristic of host–pathogen interaction is the activation of a diverse form of host-protective and stress responses, such as cell death, proliferation, and inflammation (Ashida, Ogawa, Kim, Mimuro, & Sasakawa, 2011). There are several models of host-cell death caused by pathogenic microorganisms, such as apoptosis, necrosis, and pyroptosis (Fink & Cookson, 2005).

To avoid, protect, and eliminate the intestinal infection, the first step is to understand the initial host response after pathogen invasion (Fernandes et al., 2016; Hackam, Afrazi, Good, & Sodhi, 2013; Wu et al., 2016). Innate immunity depends on the expression of various specific pattern recognition receptors (PRRs) to recognize particular bacterial molecules termed pathogen-associated molecular patterns (PAMP), such as toll-like receptors (TLRs), which initiate the production of cytokines and chemokines (Lv et al., 2017). The immune function of intestinal goblet cells from mammals has been recently investigated (Pelaseyed et al., 2014). However, whether PAMP response is involved in the disruption of goblet cells induced by 3-oxo-C12-HSL, an autoinducer of QS, is still unknown. Moreover, it has been reported that inflammatory caspases (particularly caspase-1) are important for innate immune defense, and aberrant activation of caspase-1 is associated with many auto-inflammatory diseases as well as metabolic disorders (Henao-Mejia, Elinav, Thaiss, & Flavell, 2014; Lamkanfi & Dixit, 2014). Activation of caspase-1 is crucial for trigger pyroptosis, which results in the maturation of interleukin (IL)-1β and IL-18 from their inactive precursors (Fink & Cookson, 2005). It has also been reported that caspase-1 plays an important role in inducing apoptosis via the activation of downstream caspase-3 signal (Li et al., 2000). Our previous study suggested that 3-oxo-C12-HSL induced severe cell death accompanied by increased of IL-1β messenger RNA (mRNA) and caspase-3 protein levels (Tao et al., 2016). However, whether caspase-1 contributes to inducing cell death by 3-oxo-C12-HSL and the relevant molecular mechanism underlying the dysfunction of 3-oxo-C12-HSL to host cells are still unclear.

The paraoxonase 2 (PON2) is widely expressed in mammalian tissues and cell types that function as hydrolyzes 3-oxo-C12-HSL to 3-oxo-C12-HSL-acid (Horke et al., 2015; Mackness et al., 2010; Marsillach et al., 2008). It has been reported that depending on its antioxidative and antiapoptotic activities, PON2 may attenuate 3-oxo-C12-HSL-mediated biological effects on host cells (Altenhofer et al., 2010; Kim et al., 2011). On the contrary, a recent study demonstrated that 3-oxo-C12-HSL-induced cell apoptosis was dependent upon PON2 activity in mouse embryonic fibroblasts (Schwarzer et al., 2015). Our previous study suggested that the PON2 inhibitor significantly reversed 3-oxo-C12-HSL-induced cell death in LS174T cells (Tao et al., 2016); however, the relevant signal pathway and molecular mechanism were unknown. Therefore, the aim of this study was to investigate the cellular and molecular mechanisms, particularly focused on the oxidative stress, innate immune response, and the signaling pathway underlying the disruption of LS174T goblet cells exposed to 3-oxo-C12-HSL in vitro.

2 | MATERIALS AND METHODS

2.1 | Cell culture and treatment

The human colonic differentiated LS174T goblet cells have been described previously (Hasnain et al., 2013; Tao et al., 2016) and treated with 3-oxo-C12-HSL (Sigma-Aldrich, St. Louis, MO), PON2 inhibitor (TQ416, ChemDiv, San Diego), ROS scavenger (N-acetyl-L-cysteine, Sigma-Aldrich, St. Louis, MO), the caspase-1 inhibitor (VX-765, Selleck, Shanghai, China), the caspase-3 inhibitor (Z-DEVD-FMK, Selleck, Shang Hai, China), and the NF-κB transcriptional activity inhibitor (JSH-23, Selleck, Shang Hai, China) according to the concentrations specified in the figure legends. The concentrations of all of the tested pharmacological inhibitors did not show any significant cytotoxic effects in each experiment.

2.2 | Measurement of intracellular ROS

Intracellular ROS in LS174T cells were measured with 2′,7′-dichlorofluorescein diacetate (DCFH-DA; Sigma) as a previously reported method (Gan et al., 2015). In brief, after dilution to a final concentration of 10 μM with serum-free RPMI1640, DCFH-DA was added to the cells after the culture medium was removed and incubated for 30 min at 37°C. Next, the cells were washed three times with phosphate-buffered saline (PBS). The cells were resuspended in PBS, and the fluorescence intensity was measured for more than 10,000 cells of each sample by a FACSVerse flow cytometer. The level of total intracellular ROS, paralleled by an

increase in fluorescence intensity, was calculated as the percentage of control cells.

2.3 | Annexin V externalization

The detection of annexin V externalization in LS174T cells was done as described previously (Lee et al., 2015). In brief, the cells were detached with 0.05% trypsin/EDTA, and 1×10^5 cells were resuspended with annexin V binding buffer. The cells were then stained with annexin V (25 μg/ml) and propidium iodide (PI) (125 ng/ml) and incubated for 15 min at room temperature in the dark. The sample was analyzed using a FACSVerse flow cytometer (BD Biosciences).

2.4 | 2.4. DNA fragmentation

DNA fragmentation in LS174T cells was measured with a one-step TUNEL apoptosis assay kit (Beyotime, China) according to the manufacturer's instructions.

2.5 | Cell viability assay

LS174T (5×10^4 cells/well) were cultured for 24 hr in 96-well plates. After treatment, 10 μl of the CCK-8 assay solution (Jiancheng Bioengineering Institute, Nanjing, China) was added to each well and incubated for another 1 hr. Then, the optical densities were read on a microplate reader (Molecular Devices, Sunnyvale, CA) at 450 nm. Cell viability was calculated relative to the DMSO control group. All tests were performed six times.

2.6 | Detection of malondialdehyde (MDA), H_2O_2, caspase-1, and caspase-3 activity

Cell extracts were prepared by sonication (Sonics VCX105) in ice-cold PBS and centrifuged at 12,000 rpm for 20 min to remove debris. The supernatant fluid was collected, and MDA and H_2O_2 levels were determined according to the manufacturer's instructions using commercially available kits (Shanghai Enzyme-linked Biotechnology Co. Ltd, Shanghai, China). Caspase-1 activity was measured by a previously reported method (Luo et al., 2014) using commercially available kits (Beyotime, China). Caspase-3 activity was measured using commercially available kits (Jiancheng Bioengineering Institute, Nanjing, China). The total protein concentration was determined using a BCA protein assay kit (Pierce Thermo Scientific). The data were expressed as nanomoles of MDA or H_2O_2 per milligram of protein.

2.7 | Measurement of cytokine

The levels of IL-8, IL-1β, IL-6, TNF-α, and IL12P70 in the cellular supernatant were determined using commercial kits purchased from BD Biosciences (Catalog no.: 551811), following the manufacturer's instructions.

2.8 | RNA extraction, reverse transcription, and real-time quantitative PCR

Messenger RNA extraction and reverse transcription were conducted using the SuperScript III First-Strand Synthesis System (Invitrogen), according to the manufacturer's protocol. The synthesized complementary DNA was used for quantitative real-time polymerase chain reaction (PCR). Real-time PCR was performed with Mx3000P (Stratagene). The sequences of primers used in real-time PCR are as follows: TLR1 forward primer: 5′-GGGTCAGCTGG ACTTCAGAG-3′ and backward primer: 5′-GCTAATTTTGGATGGGC AAA-3′; TLR2 forward primer: 5′-CCTCCAATCAGGCTTCTCTG-3′, and backward primer: 5′-TCCTGTTGTTGGACAGGTCA-3′; TLR3 forward primer: 5′-AGCCTTCAACGACTGATGCT-3′, and backward primer: 5′-TTTCCAGAGCCGTGCTAAGT-3′; TLR4 forward primer: 5′-TGAGCAGTCGTGCTGGTATC-3′, and backward primer: 5′-CAG GGCTTTTCTGAGTCGTC-3′; TLR5 forward primer: 5′-GAGCCCCTA CAAGGGAAAAC-3′, and backward primer: 5′-TGCTGATGGCATTGC TAAAG-3′; TLR6 forward primer: 5′-AGGGCTGGCCTGATTCTTA T-3′, and backward primer: 5′-TGGCACACCATCCTGAGATA-3′; GAPDH forward primer: 5′-TGCACCACCAACTGCTTAGC-3′, and backward primer: 5′-GGCATGGACTGTGGTCATGAG-3′. The $2^{-\Delta\Delta Ct}$ method was used to analyze the real-time PCR data. All data were normalized against the house-keeping gene GAPDH and expressed as the fold difference relative to the mean of relevant control samples.

2.9 | Preparation of cellular lysates for western blot analysis

LS174T cells were solubilized in cell lysis buffer containing 1%Triton X-100, 10 mM Tris (pH 7.4), 1 mM EDTA, 1 mM ethylene glycol tetraacetic acid (EGTA), 150 mM NaCl, and a proteinase inhibitor mixture (Roche Applied Science) and incubated for 1 hr on ice. The scraped suspensions were centrifuged at 14,000 rpm for 15 min at 4°C, and the protein concentration was determined using a BCA protein assay kit (Pierce Thermo Scientific). After denaturation by boiling for 5 min, 40 μg of protein was separated by 10% or 15% sodium dodecyl sulfate polyacrylamide gel electropheresis (SDS-PAGE), transferred on to nitrocellulose membrane (BioTrace, Pall Co), blocked with 5% bovine serum albumin (BSA) in Tris buffer (pH 7.5) with 0.1% Tween 20 for 2 hr, then incubated overnight at 4°C with anticaspase-1 (1:200, sc-515, Santa Cruz, CA), anti-IL-1β (1:200, sc-7884, Santa Cruz, CA), anti-TLR2 (1:1000, #13744, CST Technology Inc., MA), anti-TLR4 (1:1000, #14358, CST Technology Inc., MA), anti-NF-κB (1:200, sc-372, Santa Cruz, CA), anti-p-NF-κB (1:200, sc-33020, Santa Cruz, CA), anti-GSDMD (1:1000, ab210070, Abcam, UK), anti-PON2 (1:1000, ab183710, Abcam, UK), or anti-active-caspase-3 (1:1000, ab32042, Abcam, UK) antibodies. Then, the blots were incubated with the goat anti-rabbit HRP-conjugated secondary antibodies (1:10,000; BS13278, Bioworld Technology Inc.) in dilution buffer for 2 hr at 25°C. Finally, the blot was washed and detected by enhanced chemiluminescence's (ECL) using the LumiGlo substrate (Super Signal West Pico Trial Kit, Pierce), and the

signals were recorded by an imaging System (Bio-Rad) and analyzed with Quantity One software (Bio-Rad). α-tubulin (1:10,000; BS1699, Bioworld Technology Inc.) was used as a loading control for the western blot. The protein content was expressed as the fold change relative to the mean value of the control group.

2.10 | Periodic acid-schiff (PAS) and alcian blue staining

The PAS and alcian blue staining in LS174T cells were done as a previously reported method (Tao et al., 2016). In brief, after the culture medium was removed, the cells were fixed in 4% paraformaldehyde at 4°C overnight and stained using a PAS kit (Sigma-Aldrich) and alcian blue solution (Sigma-Aldrich), according to the manufacturer's instructions.

2.11 | Statistical analysis

All statistical procedures were computed using statistical software SPSS (SPSS version 11.0 for Windows; SPSS Inc., Chicago, IL). Data are presented as means ± SEM. The data were tested for normal distribution, and statistical significance was assessed by an independent sample *t* test. A *p*-value of <0.05 was considered statistically significant.

3 | RESULTS

3.1 | 3-oxo-C12-HSL induced oxidative stress in LS174T cells

As shown in Figure 1a,b, 3-oxo-C12-HSL significantly increased ROS production in a concentration-dependent manner ($p < 0.05$). The intracellular ROS level was significantly increased in LS174T cells exposed to 10–200 μM 3-oxo-C12-HSL for 4 hr (Figure 1a). Exposure time also had a significant impact on cellular ROS production. When LS174T cells were treated with 100 μM 3-oxo-C12-HSL for 1 hr to 6 hr, the level of cellular ROS was markedly increased and reached the maximum level at 4 hr of exposure ($p < 0.05$) (Figure 1b). Moreover, the level of cellular MDA and H_2O_2 was also greatly increased by 100 μM 3-oxo-C12-HSL treated for 4 hr in LS174T cells (Figure 1c,d). These results indicate an obvious oxidative stress induced by 100 μM 3-oxo-C12-HSL treated for 4 hr in LS174T goblet cells.

3.2 | Changes of caspase-1 and cytokines in LS174T cells induced by 3-oxo-C12-HSL

To investigate whether the pyroptosis pathway was involved in the damages of 100 μM 3-oxo-C12-HSL to LS174T cells for 4 hr, the level of procaspase-1 protein and the activity of caspase-1, as well as cellular IL-1β protein and several other cytokines were measured. The results showed that the level of cellular procaspase-1 protein was significantly decreased, whereas the activity of caspase-1 was markedly increased in LS174T cells treated with 3-oxo-C12-HSL ($p < 0.05$) (Figure 2a). There was no obvious change in cellular IL-1β protein expression in LS174T cells after 3-oxo-C12-HSL treatment (Figure 2b). Moreover, the marker of pyroptosis, GSDMD protein expression, also remained unchanged after 3-oxo-C12-HSL treatment of LS174T cells (Figure 2c). In addition, the level of IL-1β and several other cytokines including IL-8, TNF-α, and IL12P70 in the supernatant fraction was significantly changed by 3-oxo-C12-HSL. Unexpectedly, the concentration of IL-1β, TNF-α, and IL12P70 in the supernatant was significantly decreased ($p < 0.05$), whereas IL-8 concentration was greatly increased by 3-oxo-C12-HSL treatment ($p < 0.05$) (Figure 2d).

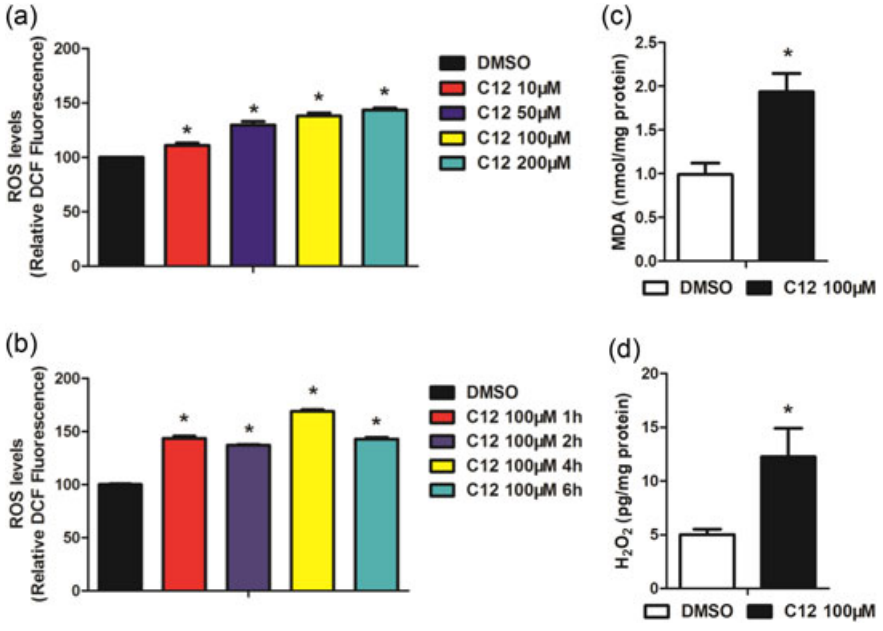

FIGURE 1 Effects of 3-oxo-C12-HSL on intracellular ROS, MDA, and H_2O_2 levels in LS174T cells. Levels of (a), (b) ROS, (c) MDA, and (d) H_2O_2 were assayed as described under Materials and Methods. Data are presented as means ± SEM of three independent experiments. *$p < 0.05$ versus DMSO group [Color figure can be viewed at wileyonlinelibrary.com]

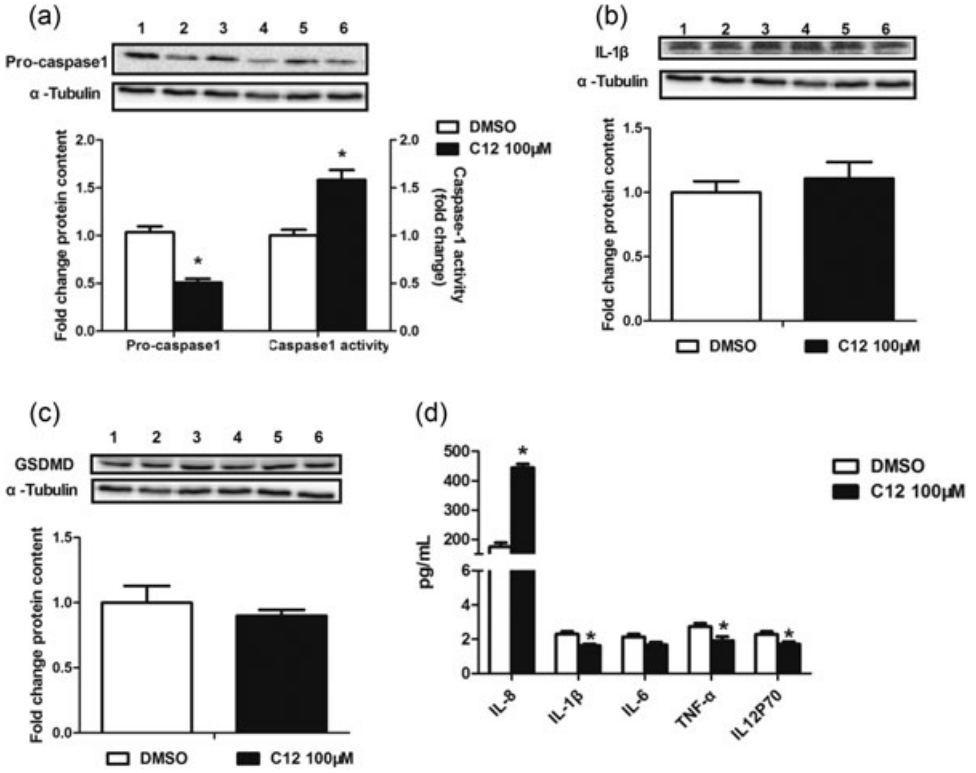

FIGURE 2 Effects of 3-oxo-C12-HSL on caspase-1 and inflammatory-relative cytokines expression in LS174T cells. LS174T cells were incubated with 3-oxo-C12-HSL (100 μM) for 4 hr. Cells were harvested and assayed for (a) pro-caspase-1 protein expression and caspase-1 activity, (b) IL-1β protein expression, (c) GSDMD protein expression, and (d) inflammatory-relative cytokines content in cell supernatant as described under Materials and Methods. For (a), (b), and (c), lines 1–6 represent DMSO, 3-oxo-C12-HSL, DMSO, 3-oxo-C12-HSL, DMSO, and 3-oxo-C12-HSL. Data are presented as means ± SEM of three independent experiments. *$p < 0.05$ versus DMSO group

3.3 | Changes of TLRs mRNA and proteins expression in LS174T cells induced by 3-oxo-C12-HSL

To identify the potential effect of 100 μM 3-oxo-C12-HSL treated for 4 hr on the innate immune response in LS174T cells, the expression of TLRs mRNA and proteins was detected by real-time PCR and western blot analysis, respectively. The results demonstrated that TLR2, 3 and 4 mRNA expression were significantly upregulated by 3-oxo-C12-HSL ($p < 0.05$), yet TLR1, 5 and 6 mRNA expression were

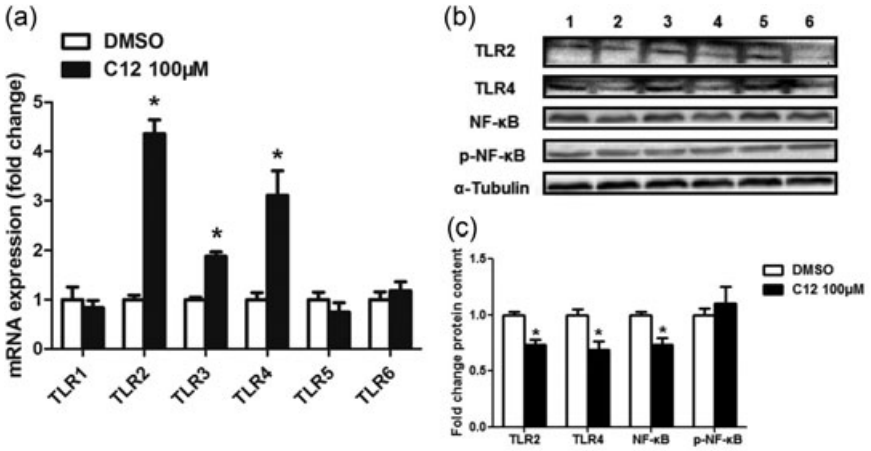

FIGURE 3 Effects of 3-oxo-C12-HSL on innate immune response pathway in LS174T cells. LS174T cells were incubated with 3-oxo-C12-HSL (100 μM) for 4 hr. Cells were harvested and assayed for (a) TLRs mRNA expression, (b) TLR2, TLR4, and NF-κB protein expression as described under Materials and Methods. For (b), lines 1–6 represent DMSO, 3-oxo-C12-HSL, DMSO, 3-oxo-C12-HSL, DMSO, and 3-oxo-C12-HSL. Data are presented as means ± SEM of three independent experiments. *$p < 0.05$ versus DMSO group

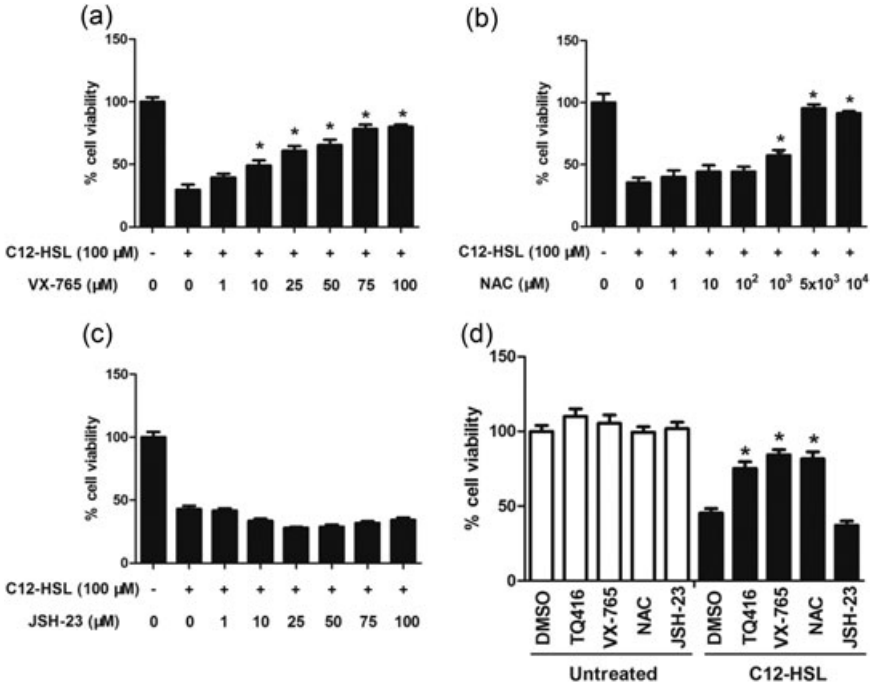

FIGURE 4 Effects of various inhibitors on viability after 3-oxo-C12-HSL treated LS174T cells. LS174T cells were seeded at a density of 5×10^4/well in 96-well plates. Cells viability were assayed for (a) cells were incubated with 3-oxo-C12-HSL and VX-765 together for 4 hr, (b) cells were pretreatment with NAC for 1 hr and then incubated with 3-oxo-C12-HSL and NAC together for an additional 4 hr, (c) cells were incubated with 3-oxo-C12-HSL and JSH-23 together for 4 hr, and (d) LS174T cells were incubated with TQ416 (1 μM), VX-765 (100 μM), or JSH-23 (50 μM) together with 3-oxo-C12-HSL (100 μM) for 4 hr or pretreatment with NAC (5 mM) for 1 hr and then incubated with 3-oxo-C12-HSL (100 μM) and NAC (5 mM) together for an additional 4 hr. Data are presented as means ± SEM of six independent experiments. *$p < 0.05$ versus 3-oxo-C12-HSL treatment group

not altered ($p > 0.05$) (Figure 3a). In contrast, the level of TLR2 and TLR4 protein showed a significant decrease by 3-oxo-C12-HSL treatment (Figure 3b,c). In addition, the total abundance of NF-κB protein was also significantly decreased ($p < 0.05$), whereas the level of phosphorylated NF-κB (p- NF-κB) was not significantly changed by 3-oxo-C12-HSL (Figure 3b,c).

3.4 | The rescuing effects of several inhibitors on cell viability in 3-oxo-C12-HSL-treated LS174T cells

The damage of 3-oxo-C12-HSL to cell viability has been determined in our previous study (Tao et al., 2016). To reveal whether caspase-1, oxidative stress, and NF-κB pathway were involved in the process of 100 μM 3-oxo-C12-HSL-induced LS174T cell damage, the rescue effect of caspase-1 inhibitor VX-765, antioxidant NAC, as well as NF-κB pathway inhibitor JSH-23 on cell viability was evaluated in this study. VX-765 at a concentration range of 10–100 μM or NAC at a concentration range of 1–10 mM can remarkably rescue cell viability damage upon 3-oxo-C12-HSL treatment in LS174T cells (Figure 4a,b). However, NF-κB pathway inhibitor JSH-23 at the range of 1–100 μM concentration did not show an obvious effect on cell viability after being cotreated with 3-oxo-C12-HSL (Figure 4c). TQ416, an inhibitor of PON2, was confirmed to exhibit a positive effect on rescuing cell viability when cotreated with 3-oxo-C12-HSL (Figure 4d).

3.5 | Effects of several inhibitors on oxidative stress in 3-oxo-C12-HSL-treated LS174T cells

The level of cellular ROS and H_2O_2, as well as MDA, was significantly increased in LS174T cells when exposed to 100 μM 3-oxo-C12-HSL for 4 hr, which could be reduced by TQ416, NAC, and VX-765 and almost returned to the normal level. However, JSH-23, a NF-κB pathway inhibitor, did not show a positive effect on the production of these oxidative parameters (Figure 5a–c). Our data collectively suggest that TQ416, VX-765, and NAC can eliminate the oxidative stress induced by 100 μM 3-oxo-C12-HSL to LS174T cells for 4 hr.

3.6 | Signal pathways involved in regulating cytokines secretion in 3-oxo-C12-HSL-treated LS174T cells

The level of cytokines was measured in the medium of LS174T cells culture treated with 100 μM 3-oxo-C12-HSL alone or with inhibitors. We found that 100 μM 3-oxo-C12-HSL markedly increased the secretion of IL-8 after 4-hr treatment, and TQ416, VX-765 and NAC significantly blocked the increase of IL-8 secretion induced by 3-oxo-C12-HSL in

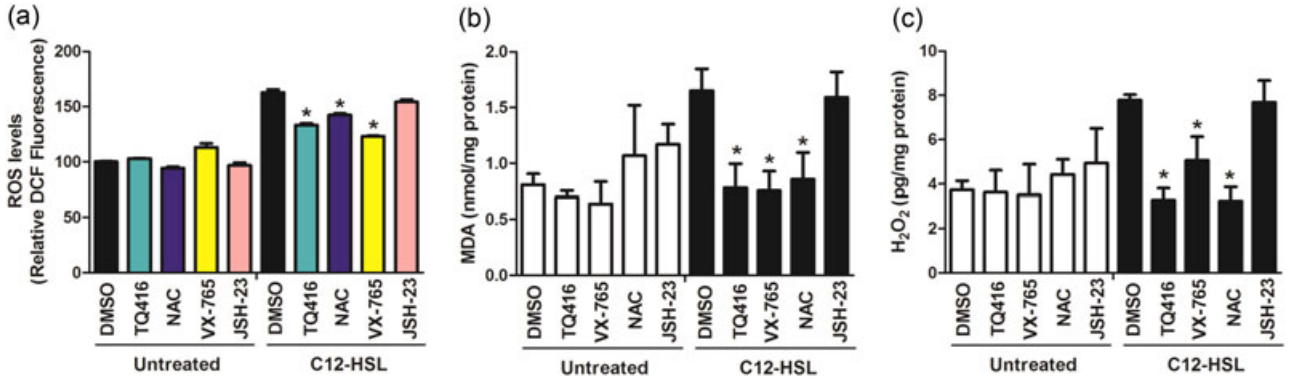

FIGURE 5 Effects of various inhibitors on intracellular ROS, MDA, and H_2O_2 levels after 3-oxo-C12-HSL treated LS174T cells. LS174T cells were incubated with TQ416 (1 μM), VX-765 (100 μM), or JSH-23 (50 μM) together with 3-oxo-C12-HSL (100 μM) for 4 hr or pretreatment with NAC (5 mM) for 1 hr and then incubated with 3-oxo-C12-HSL and NAC together for an additional 4 hr. Levels of (a) ROS, (b) MDA, and (c) H_2O_2 were assayed as described under Materials and Methods. Data are presented as means ± SEM of three independent experiments. $^*p < 0.05$ versus 3-oxo-C12-HSL treatment group [Color figure can be viewed at wileyonlinelibrary.com]

LS174T cells ($p < 0.05$) (Figure 6a). Unexpectedly, the level of other cytokines, including IL-1β, TNF-α and IL12P70, in the supernatant was significantly decreased by 3-oxo-C12-HSL treatment, and the TQ416, VX-765 and NAC could further decrease the secretion of these cytokines from LS174T cells when cotreated with 3-oxo-C12-HSL (Figure 6b–e).

3.7 | Caspase-1 activity in 3-oxo-C12-HSL-treated LS174T cells

Caspase-1 plays a critical role in mediating the sterile inflammation initiated by endogenous danger signals and eventually leads to cell apoptosis. To explore whether oxidative stress results in the

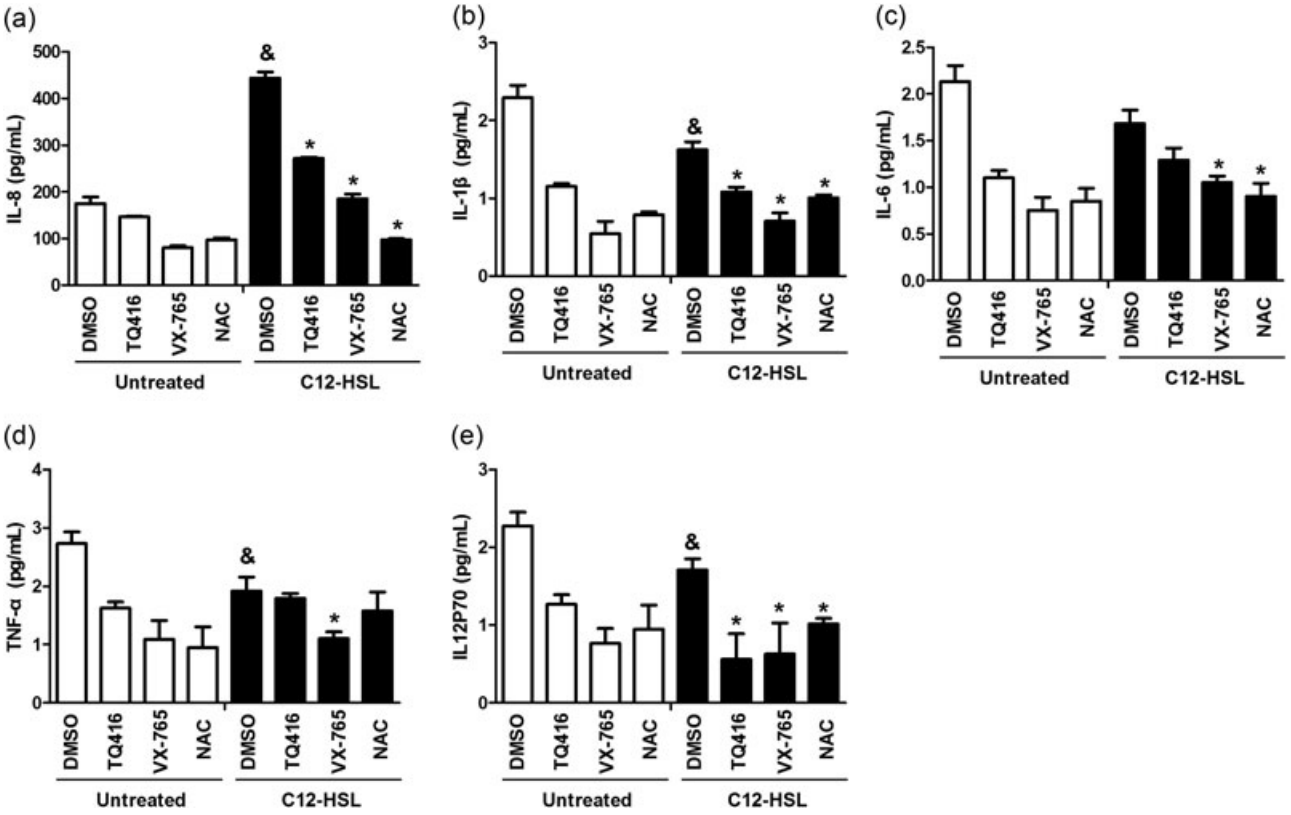

FIGURE 6 Effect of variant inhibitors on cytokines secretion in 3-oxo-C12-HSL-treated LS174T cells. LS174T cells were incubated with TQ416 (1 μM), VX-765 (100 μM) or JSH-23 (50 μM) together with 3-oxo-C12-HSL for 4 hr or pretreatment with NAC (5 mM) for 1 hr and then incubated with 3-oxo-C12-HSL and NAC together for an additional 4 hr. Levels of cytokines were assayed as described under Materials and Methods. Data are presented as means ± SEM of three independent experiments. $^{\&}p < 0.05$ versus DMSO control group. $^*p < 0.05$ versus 3-oxo-C12-HSL treatment group

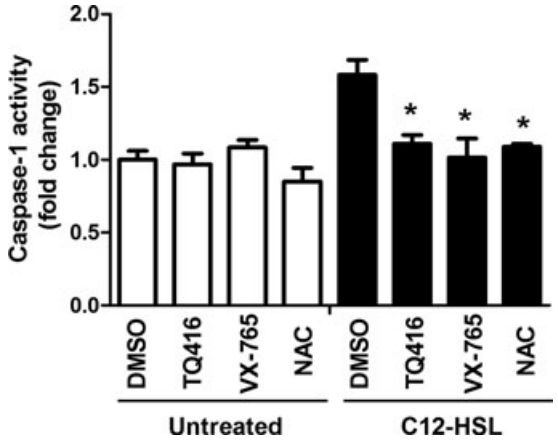

FIGURE 7 Effects of various inhibitors on caspse1 activity after 3-oxo-C12-HSL treated LS174T cells. LS174T cells were incubated with TQ416 (1 μM), VX-765 (100 μM), or JSH-23 (50 μM) together with 3-oxo-C12-HSL for 4 hr or pretreated with NAC (5 mM) for 1 hr and then incubated with 3-oxo-C12-HSL and NAC together for an additional 4 hr. Cells were harvested and assayed for capase1 activity in cell supernatant as described under Materials and Methods. Data are presented as means ± SEM of three independent experiments. $^{\&}p < 0.05$ versus DMSO control group. $^{*}p < 0.05$ versus 3-oxo-C12-HSL treatment group

activation of caspase-1, caspase-1 activity was determined in LS174T cells treated with 100 μM 3-oxo-C12-HSL alone or combined with inhibitors. The results showed that 100 μM 3-oxo-C12-HSL remarkably increased caspase-1 activity, and TQ416, VX-765, and NAC could significantly inhibit the activation of caspase-1 activity induced by 3-oxo-C12-HSL ($p < 0.05$) (Figure 7).

3.8 | Caspase-3 involved in the damage of 3-oxo-C12-HSL to LS174T cells

As one of the downstream of caspases, caspase-3 acts as the final effector to induce cell death. To determine whether caspase-3 mediates C12-HSL-induced LS174T cells damage, we tested the effect of the caspase-3 inhibitor Z-DEVD-FMK on C12-HSL-induced cell apoptosis and oxidative impairment. When used at a concentration range of 0–100 μM, Z-DEVD-FMK remarkably rescued C12-HSL-induced cell viability (Figure 8a). Further analysis demonstrated that 75 μM Z-DEVD-FMK significantly reversed C12-HSL-induced apoptotic cell death (Figure 8b), inhibited DNA fragmentation (Figure 8e) in LS174T cells.

Moreover, TQ416, VX-765, and NAC also can inhibit the caspase-3 activity and protein expression initiated by 3-oxo-C12-HSL (Figure 6c, d). A significant decrease of ROS production was also obviously observed in LS174T cells after treatment with Z-DEVD-FMK (Figure 8f).

3.9 | Mucin synthesis and sulfation in 3-oxo-C12-HSL-treated LS174T cells

PAS and alcian blue staining were performed to evaluate the level of mucous glycoprotein and sulfation. The secretion and sulfation of mucin were significantly decreased by 100 μM 3-oxo-C12-HSL in LS174T cells; but cotreatment with VX-765 and Z-DEVD-FMK showed a significant rescuing effect on mucin secretion and sulfation (Figure 9a,b). These results indicate that caspase-1 and 3 were involved in the damages of 3-oxo-C12-HSL to mucoprotein synthesis and sulfation in LS174T cells.

4 | DISCUSSION

As the first-line defensive barrier of gut, the mucus layer plays a key role against invading microbes and pathogenic antigens (Ivanov, Parkos, & Nusrat, 2010). Mucin 2 (Muc 2), a glycoprotein synthesized by goblet cells, is the major composition of the mucus layer (Wickens & Cox, 2009). The disruption of Muc 2 leads to the inflammatory bowel diseases induced by various intestinal infections such as bacteria, viruses, and parasites (Hansson, 2012; Shirazi, Longman, Corfield, & Probert, 2000). Many studies have reported that 3-oxo-C12-HSL, one of QS molecules produced by Gram-negative bacteria in the gastrointestinal tract, can damage the intestinal barrier and induce the secretion of cytokines and cell migration (Karlsson, Turkina, Yakymenko, Magnusson, & Vikström, 2012; Smith et al., 2001; Vikstrom, Tafazoli, & Magnusson, 2006; Vikstrom, Bui, Konradsson, & Magnusson, 2009; Vikstrom et al., 2010). Our previous study demonstrated that 3-oxo-C12-HSL could rapidly trigger the mitochondrial dysfunction, and lead to the decrease of both cell viability and Muc 2 production in LS174T cells (Tao et al., 2016). In this study, the cellular and molecular mechanisms behind the damages caused by 3-oxo-C12-HSL on goblet cells were further investigated. Our data collectively showed that 3-oxo-C12-HSL induces the production of ROS and the activation of caspase-1-dependent apoptosis, which eventually results in cell death and functional disorders of mucin secretion from LS174T goblet cells.

In a physiological context, ROS are produced as a natural byproduct of the normal metabolism of cells and play important roles in cell homeostasis. However, during times of environmental stress, ROS levels can increase dramatically, which may cumulatively induce an oxidative stress and eventually result in significant damages to cell structures and functions (Bruns, Peter, Hagel, Herrmann, & Stallmach, 2011; Dey & Bishayi, 2015; Gan et al., 2015; Zheng et al., 2016). A previous study reported that the concentrations of 3-oxo-C12-HSL can reach 300–600 μM in *Pseudomonas aeruginosa* biofilms (Charlton et al., 2000). We examined the effects of 3-oxo-C12-HSL in the range of 0–200 μM on oxidative stress status of LS174T cells. Our data showed that the cellular ROS levels (quantified by flow cytometry via staining cells with DCFH-DA) increased markedly in LS174T cells after treatment with 100 μM 3-oxo-C12-HSL for 4 hr, indicating an oxidative stress induced by 3-oxo-C12-HSL. Therefore, we used this concentration to performed subsequent experiments.

Previous studies have suggested that PON2 is widely expressed in many cell types, independent of its hydrolytic activity, PON2 has antioxidant anti-inflammatory and antiapoptotic activities in HAEC

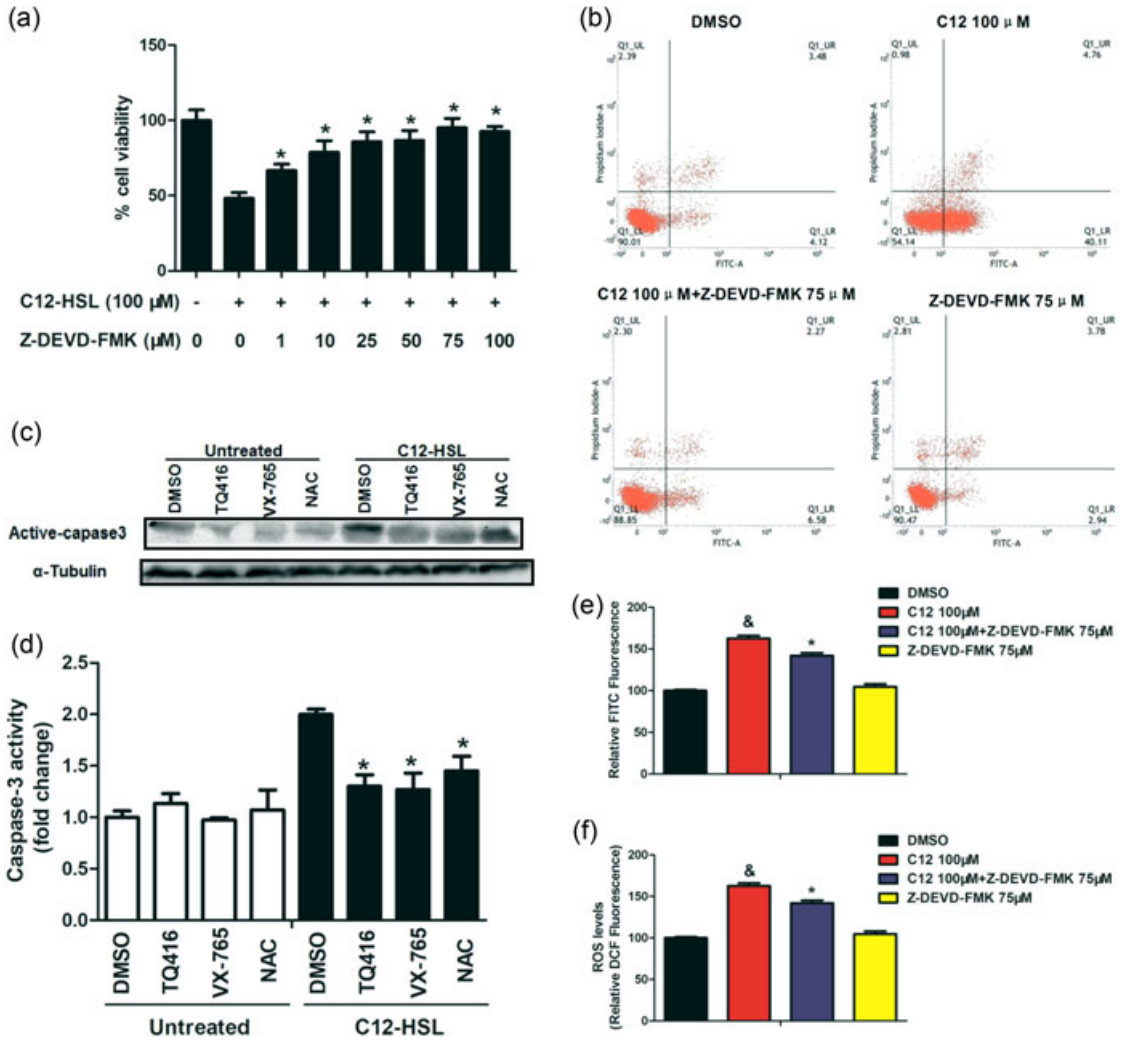

FIGURE 8 Effects of caspase-3 on cell viability, apoptosis and intracellular ROS after 3-oxo-C12-HSL treated LS174T cells. LS174T cells were incubated with 3-oxo-C12-HSL and Z-DEVD-FMK for 4 hr. Cells were harvested and assayed for (a) cells viability, (b) annexin V externalization, (c) active-caspase-3 protein expression, (d) caspase-3 acitivity, (e) DNA fragmentation, and (f) ROS. Data are presented as means ± SEM of six independent experiments for (a) and three independent experiments for others. $^{\&}p < 0.05$ versus DMSO control group. $^{*}p < 0.05$ versus 3-oxo-C12-HSL treatment group [Color figure can be viewed at wileyonlinelibrary.com]

cells (Kim et al., 2011). However, a recent study demonstrated that 3-oxo-C12-HSL-induced cell apoptosis was dependent on PON2 hydrolytic activity (Schwarzer et al., 2015). In addition, Horke et al. (2015) demonstrated a novel PON2-dependent mechanism, by which 3-oxo-C12-HSL elicits biological effects in mammalian cells. Consistent with Horke's study, our study demonstrated that the oxidative stress, cytokines expression, and cell apoptosis were induced by 3-oxo-C12-HSL with a higher level of ROS, IL-8, and apoptotic cells, and these biological effects can be inhibited by TQ416 (PON2 inhibitor) in LS174T cells.

Previous studies have demonstrated that various virulence molecules induced pyroptosis via oxidative stress in mammal cells (Jang et al., 2015; Ren, Wu, Jiang, Hao, & Liu, 2016). Thus, we wanted to investigate whether pyroptosis mediated by high amounts of ROS was involved in the damage of cell viability of 3-oxo-C12-HSL to LS174T cells. Our data showed that the level of procaspase-1 protein was significantly reduced, whereas its enzyme activity was markedly elevated. However, we did not find a significant change of IL-1β generation or secretion from LS174T cells. Moreover, GSDMD (a new marker of pyroptosis) protein expression also remained unchanged after treatment of LS174T cells with 3-oxo-C12-HSL. Much evidence has shown that caspase-1 processes the proinflammatory cytokine pro-IL-1β to generate mature IL-1β, which is presumably released by cell lysis during pyroptosis (Rathinam & Fitzgerald, 2016). Thus, it's reasonable for us to speculate that the obvious cell death induced by 3-oxo-C12-HSL did not rely on the classic pyroptosis pathway. Nevertheless, our data showed that VX-765, a specific inhibitor of caspase-1, could inhibit the decrease of the viability of LS174T cells induced by 3-oxo-C12-HSL. This result indicates that caspase-1 cascade has been at least partially involved in the damage process of 3-oxo-C12-HSL to LS174T cells. It has been reported that oxidative stress induced caspase-1 activation (Abais, Xia, Zhang,

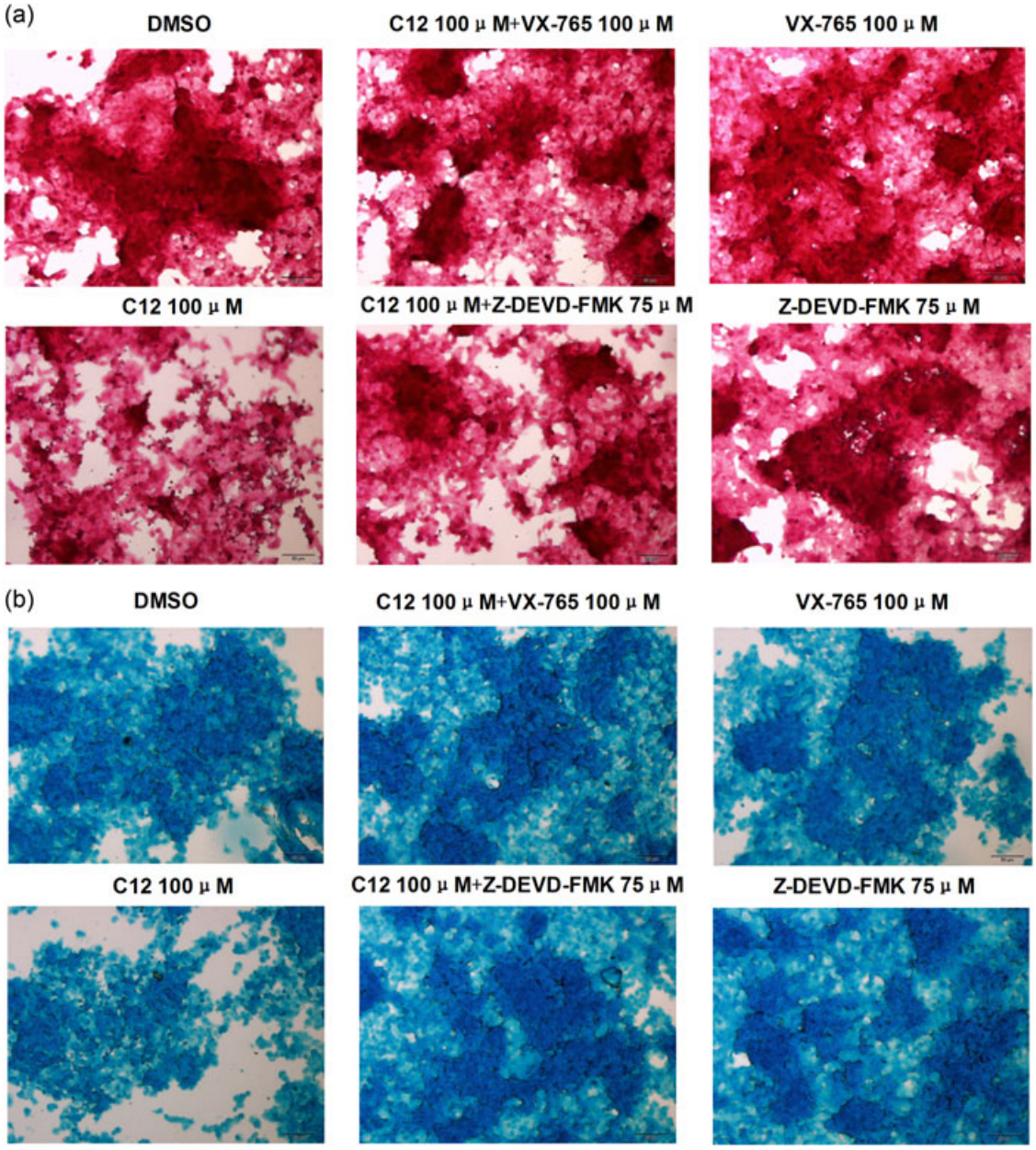

FIGURE 9 Effects of VX-765 and Z-DEVD-FMK on mucoprotein synthesis and sulfation in 3-oxo-C12-HSL-treated LS174T cells. LS174T cells were incubated with VX-765 (100 μM) or Z-DEVD-FMK (75 μM) together with 3-oxo-C12-HSL for 4 hr. Cells were harvested and assayed for (a) PAS staining and (b) alcian blue staining. Scale bar = 50 μm [Color figure can be viewed at wileyonlinelibrary.com]

Boini, & Li, 2015; Lee et al., 2015). Similarly, in this study, we proposed that the activation of caspase-1 induced by 3-oxo-C12-HSL was mediated by the increase of the intracellular redox levels. Therefore, we used the antioxidant NAC targeting to decrease ROS levels, as described in a previous report (Patten et al., 2013). As expected, the results showed that pretreatment with NAC significantly inhibited the increase of ROS, MDA, and H_2O_2 levels induced by 3-oxo-C12-HSL, and simultaneously alleviated the activation of caspase-1. Taken together, our data strongly support that the cell death induced by 3-oxo-C12-HSL in LS174T cells is at least partially mediated by the caspase-1 signal pathway, and pyroptosis might be not involved in this biological process.

It is well known that the caspase-3 is an executioner of cell apoptosis (Chin, Flynn, Fedwick, & Buret, 2006; Yue, Ma, Zhao, Li, & Li, 2012). In this study, Z-DEVD-FMK, a specific caspase-3 inhibitor, was used to evaluate the importance of caspase-3 in the process of 3-oxo-C12-HSL-mediated damages to LS174T cells. Our data showed that Z-DEVD-FMK can significantly restore the viability of LS174T cells by preventing cell apoptosis and cellular ROS production. Caspase-1 was identified as the IL-1-converting enzyme and is now classified as a cytokine processor caspase, along with caspase-4, 5, and 11 (Shi et al., 2014; Shi et al., 2015). Even though the major role of caspase-1 has been to mediate cytokine processing, a role for caspase-1 as an inducer of apoptosis has also been postulated (Li et al., 2000). Next, we evaluated

whether caspase-1 mediated the activation of caspase-3 in 3-oxo-C12-HSL-treated LS174T cells. It is very interesting to note that VX-765, the specific inhibitor of caspase-1, significantly inhibited the activation of the active-caspase-3 protein expression induced by 3-oxo-C12-HSL in LS174T cells. Moreover, both VX-765 and Z-DEVD-FMK, the specific inhibitors of caspase-1 and 3, can markedly rescue the synthesis and mature sulfation of mucous glycoprotein secretion from LS174T cells exposed to 3-oxo-C12-HSL. These results strongly suggest that the dysfunction of mucin production induced by 3-oxo-C12-HSL to LS174T cells largely depends on caspase-1 and 3 cascade signals.

The human gut harbors a diverse population of nonpathogenic, commensal bacteria whose contribution to gastrointestinal health and disease is now recognized (Kelly & Conway, 2005). Microorganisms that invade a vertebrate host are initially recognized by the innate immune system through germ line-encoded PRRs. Several classes of PRRs, including Toll-like receptors, function in microbial recognition and directly activate inflammatory process (Akira, Uematsu, & Takeuchi, 2006). In the current study, we detected the mRNA and protein expression of TLRs in LS174T cells under 3-oxo-C12-HSL exposure. The mRNA expression results suggest that the level of TLR2, 3, and 4 mRNA expressions was markedly increased in LS174T cells induced by 3-oxo-C12-HSL exposure. Among these TLRs, the induction of TLR2 and TLR4 was particularly susceptible to 3-oxo-C12-HSL treatment; thus we further detected the protein expression of TLR2, TLR4, and transcription factor NF-κB in LS174T cells. Conversely, the level of TLR2, TLR4, and NF-κB was significantly downregulated by 3-oxo-C12-HSL. The increase of mRNA abundance, but a decrease in their proteins contents, indicated a posttranscriptional regulation mechanism, such as the degradation function of microRNA. Besides, the level of phosphorylated NF-κB protein did not show a significant change by 3-oxo-C12-HSL. Moreover, JSH-23, an inhibitor of NF-κB transcription activity did not show a positive effect for alleviating the oxidative stress or rescuing cell viability in 3-oxo-C12-HSL treated LS174T cells. These results suggested that the changes in TLRs expression did not induce changes in NF-κB the downstream signal, and the blockade NF-κB signal pathway did not produce a positive effect on LS174T cell when exposed to 3-oxo-C12-HSL. These data indicate that the TLRs-NF-κB pathway might not be involved in the damaged process induced by 3-oxo-C12-HSL to LS174T cells. The biological significance behind the significant changes of TLRs expression induced by 3-oxo-C12-HSL still needs further investigation.

We also detected the inflammatory cytokines in the supernatant in 3-oxo-C12-HSL-treated LS174T cells. Unexpectedly, the level of most cytokines including IL-1β, TNF-α, and IL12P70 was significantly decreased, and the level of cytokines was further decreased by cotreatment with inhibitors of TQ416, NAC, and VX-765. However, it is very important to note that the level of IL-8 was greatly increased by 3-oxo-C12-HSL. A previous study suggested that 3-oxo-C12-HSL-induced production of IL-8 was transcriptionally regulated by NF-κB (Smith et al., 2001); however, the signal pathway of NF-κB was not altered by 3-oxo-C12-HSL in the current study. Moreover, we found that the increase of IL-8 induced by 3-oxo-C12-HSL was inhibited after cotreatment of TQ416, NAC, VX-765, and 3-oxo-C12-HSL in LS174T cells. Unfortunately, no data or references are available for explaining the effects of 3-oxo-C12-HSL with or without the inhibitors on cellular cytokines generation or secretion. Although the significant decrease in IL-1β, TNF-α, and IL12P70 levels in 3-oxo-C12-HSL-treated LS174T cells was obscure, it is reasonable to propose that IL-8 plays a dominant role in the damage process of 3-oxo-C12-HSL to LS174T cells based on the significant changes of IL-8 induced by 3-oxo-C12-HSL alone or cotreated with the inhibitors. However, whether the activation of IL-8 is generated from pro-IL-8 under the role of caspase-1 as observed in caspase-1-IL-1β processing cascade still requries further study.

In conclusion, we report herein for the first time that 3-oxo-C12-HSL induced high oxidative stress via PON2 in LS174T goblet cells, which in turn activated the caspase-1 and 3 cascade signals, and eventually resulted in cell apoptosis and the dysfunction of mucin secretion and maturation. Innate inflammation is also involved in the adverse impacts of 3-oxo-C12-HSL to LS174T cells, cytokines particularly IL-8 may be involved in this process. Therefore, our data are useful for better understanding the mechanism behind the negative effects of QS molecules to host cells.

ACKNOWLEDGMENTS

This study was supported by the National Nature Science Foundation of China (project no. 31572433), the National Basic Research Program of China (project no. 2011CB100802), the Program for New Century Excellent Talents in University (NCET-13–0862), and a project funded by the Priority Academic Program Development of Jiangsu Higher Education Institutions (PAPD).

CONFLICTS OF INTEREST

The authors declare that they have no conflicts of interest.

ORCID

Shiyu Tao http://orcid.org/0000-0003-2600-3309

REFERENCES

Abais, J. M., Xia, M., Zhang, Y., Boini, K. M., & Li, P. L. (2015). Redox regulation of NLRP3 inflammasomes: ROS as trigger or effector. *Antioxidants & Redox Signaling*, *22*(13), 1111–1129.

Akira, S., Uematsu, S., & Takeuchi, O. (2006). Pathogen recognition and innate immunity. *Cell*, *124*(4), 783–801.

Altenhöfer, S., Witte, I., Teiber, J. F., Wilgenbus, P., Pautz, A., Li, H., … Horke, S. (2010). One enzyme, two functions: PON2 prevents mitochondrial superoxide formation and apoptosis independent from its lactonase activity. *The Journal of Biological Chemistry*, *285*(32), 24398–24403.

Ashida, H., Ogawa, M., Kim, M., Mimuro, H., & Sasakawa, C. (2011). Bacteria and host interactions in the gut epithelial barrier. *Nature Chemical Biology*, *8*(1), 36–45.

Bruns, T., Peter, J., Hagel, S., Herrmann, A., & Stallmach, A. (2011). The augmented neutrophil respiratory burst in response to *Escherichia coli* is reduced in liver cirrhosis during infection. *Clinical and Experimental Immunology*, *164*(3), 346–356.

Charlton, T. S., de Nys, R., Netting, A., Kumar, N., Hentzer, M., Givskov, M., & Kjelleberg, S. (2000). A novel and sensitive method for the quantification of N-3-oxoacyl homoserine lactones using gas chromatography-mass spectrometry: Application to a model bacterial biofilm. *Environmental Microbiology*, *2*(5), 530–541.

Chin, A. C., Flynn, A. N., Fedwick, J. P., & Buret, A. G. (2006). The role of caspase-3 in lipopolysaccharide-mediated disruption of intestinal epithelial tight junctions. *Canadian Journal of Physiology and Pharmacology*, *84*(10), 1043–1050.

Dey, S., & Bishayi, B. (2015). Killing of *Staphylococcus aureus* in murine macrophages by chloroquine used alone and in combination with ciprofloxacin or azithromycin. *Journal of Inflammation Research*, *8*, 29–47.

Eum, S. Y., Jaraki, D., Bertrand, L., András, I. E., & Toborek, M. (2014). Disruption of epithelial barrier by quorum-sensing N-3-(oxododecanoyl)-homoserine lactone is mediated by matrix metalloproteinases. *American Journal of Physiology Gastrointestinal and Liver Physiology*, *306*(11), G992–G1001.

Fernandes, P., MacSharry, J., Darby, T., Fanning, A., Shanahan, F., Houston, A., & Brint, E. (2016). Differential expression of key regulators of Toll-like receptors in ulcerative colitis and Crohn's disease: A role for Tollip and peroxisome proliferator-activated receptor gamma. *Clinical and Experimental Immunology*, *183*(3), 358–368.

Fink, S. L., & Cookson, B. T. (2005). Apoptosis, pyroptosis, and necrosis: Mechanistic description of dead and dying eukaryotic cells. *Infection and Immunity*, *73*(4), 1907–1916.

Gan, F., Zhang, Z., Hu, Z., Hesketh, J., Xue, H., Chen, X., … Huang, K. (2015). Ochratoxin A promotes porcine circovirus type 2 replication in vitro and in vivo. *Free Radical Biology & Medicine*, *80*, 33–47.

Hackam, D. J., Afrazi, A., Good, M., & Sodhi, C. P. (2013). Innate immune signaling in the pathogenesis of necrotizing enterocolitis. *Clinical & Developmental Immunology*, *2013*, 475415.

Hansson, G. C. (2012). Role of mucus layers in gut infection and inflammation. *Current Opinion in Microbiology*, *15*(1), 57–62.

Hasnain, S. Z., Tauro, S., Das, I., Tong, H., Chen, A. C. H., Jeffery, P. L., … McGuckin, M. A. (2013). IL-10 promotes production of intestinal mucus by suppressing protein misfolding and endoplasmic reticulum stress in goblet cells. *Gastroenterology*, *144*(2), 357–368 e359.

Henao-Mejia, J., Elinav, E., Thaiss, C. A., & Flavell, R. A. (2014). Inflammasomes and metabolic disease. *Annual Review of Physiology*, *76*, 57–78.

Horke, S., Xiao, J., Schütz, E. M., Kramer, G. L., Wilgenbus, P., Witte, I., … Teiber, J. F. (2015). Novel paraoxonase 2-dependent mechanism mediating the biological effects of the *Pseudomonas aeruginosa* quorum-sensing molecule N-(3-oxo-dodecanoyl)-L-homoserine lactone. *Infection and Immunity*, *83*(9), 3369–3380.

Ivanov, A. I., Parkos, C. A., & Nusrat, A. (2010). Cytoskeletal regulation of epithelial barrier function during inflammation. *The American Journal of Pathology*, *177*(2), 512–524.

Ivanov, I. I., & Honda, K. (2012). Intestinal commensal microbes as immune modulators. *Cell Host & Microbe*, *12*(4), 496–508.

Jang, Y., Lee, A. Y., Jeong, S. H., Park, K. H., Paik, M. K., Cho, N. J., … Cho, M. H. (2015). Chlorpyrifos induces NLRP3 inflammasome and pyroptosis/apoptosis via mitochondrial oxidative stress in human keratinocyte HaCaT cells. *Toxicology*, *338*, 37–46.

Johansson, M. E., Sjövall, H., & Hansson, G. C. (2013). The gastrointestinal mucus system in health and disease. *Nature Reviews Gastroenterology & Hepatology*, *10*(6), 352–361.

Johansson, M. E. V., Gustafsson, J. K., Holmén-Larsson, J., Jabbar, K. S., Xia, L., Xu, H., … Hansson, G. C. (2014). Bacteria penetrate the normally impenetrable inner colon mucus layer in both murine colitis models and patients with ulcerative colitis. *Gut*, *63*(2), 281–291.

Karlsson, T., Turkina, M. V., Yakymenko, O., Magnusson, K. E., & Vikström, E. (2012). The *Pseudomonas aeruginosa* N-acylhomoserine lactone quorum sensing molecules target IQGAP1 and modulate epithelial cell migration. *PLoS Pathogens*, *8*(10), e1002953.

Kelly, D., & Conway, S. (2005). Bacterial modulation of mucosal innate immunity. *Molecular Immunology*, *42*(8), 895–901.

Kim, J. B., Xia, Y. R., Romanoski, C. E., Lee, S., Meng, Y., Shi, Y. S., … Shih, D. M. (2011). Paraoxonase-2 modulates stress response of endothelial cells to oxidized phospholipids and a bacterial quorum-sensing molecule. *Arteriosclerosis, Thrombosis, and Vascular Biology*, *31*(11), 2624–2633.

Kim, Y. S., & Ho, S. B. (2010). Intestinal goblet cells and mucins in health and disease: Recent insights and progress. *Current Gastroenterology Reports*, *12*(5), 319–330.

Lamkanfi, M., & Dixit, V. M. (2014). Mechanisms and functions of inflammasomes. *Cell*, *157*(5), 1013–1022.

Lee, S. J., Jung, Y. H., Song, E. J., Jang, K. K., Choi, S. H., & Han, H. J. (2015). *Vibrio vulnificus* VvpE stimulates IL-1beta production by the hypomethylation of the IL-1beta promoter and NF-kappaB activation via lipid raft-dependent ANXA2 recruitment and reactive oxygen species signaling in intestinal epithelial cells. *Journal of Immunology*, *195*(5), 2282–2293.

Li, L., Hooi, D., Chhabra, S. R., Pritchard, D., & Shaw, P. E. (2004). Bacterial N-acylhomoserine lactone-induced apoptosis in breast carcinoma cells correlated with down-modulation of STAT3. *Oncogene*, *23*(28), 4894–4902.

Li, M., Ona, V. O., Guegan, C., Chen, M., Jackson-Lewis, V., Andrews, L. J., … Friedlander, R. M. (2000). Functional role of caspase-1 and caspase-3 in an ALS transgenic mouse model. *Science*, *288*(5464), 335–339.

Linden, S. K., Sutton, P., Karlsson, N. G., Korolik, V., & McGuckin, M. A. (2008). Mucins in the mucosal barrier to infection. *Mucosal Immunology*, *1*(3), 183–197.

Luo, B., Li, B., Wang, W., Liu, X., Xia, Y., Zhang, C., … An, F. (2014). NLRP3 gene silencing ameliorates diabetic cardiomyopathy in a type 2 diabetes rat model. *PLoS One*, *9*(8), e104771.

Lv, S., Li, J., Qiu, X., Li, W., Zhang, C., Zhang, Z. N., & Luan, B. (2017). A negative feedback loop of ICER and NF-kappaB regulates TLR signaling in innate immune responses. *Cell Death and Differentiation*, *24*(3), 492–499.

Mackness, B., Beltran-Debon, R., Aragones, G., Joven, J., Camps, J., & Mackness, M. (2010). Human tissue distribution of paraoxonases 1 and 2 mRNA. *IUBMB Life*, *62*(6), 480–482.

Marsillach, J., Mackness, B., Mackness, M., Riu, F., Beltrán, R., Joven, J., & Camps, J. (2008). Immunohistochemical analysis of paraoxonases-1, 2, and 3 expression in normal mouse tissues. *Free Radical Biology & Medicine*, *45*(2), 146–157.

Parlato, M., & Yeretssian, G. (2014). NOD-like receptors in intestinal homeostasis and epithelial tissue repair. *International Journal of Molecular Sciences*, *15*(6), 9594–9627.

Patten, A. R., Brocardo, P. S., Sakiyama, C., Wortman, R. C., Noonan, A., Gil-Mohapel, J., & Christie, B. R. (2013). Impairments in hippocampal synaptic plasticity following prenatal ethanol exposure are dependent on glutathione levels. *Hippocampus*, *23*(12), 1463–1475.

Pelaseyed, T., Bergström, J. H., Gustafsson, J. K., Ermund, A., Birchenough, G. M. H., Schütte, A., … Hansson, G. C. (2014). The mucus and mucins of the goblet cells and enterocytes provide the first defense line of the gastrointestinal tract and interact with the immune system. *Immunological Reviews*, *260*(1), 8–20.

Rathinam, V. A. K., & Fitzgerald, K. A. (2016). Inflammasome complexes: Emerging mechanisms and effector functions. *Cell*, *165*(4), 792–800.

Ren, J. D., Wu, X. B., Jiang, R., Hao, D. P., & Liu, Y. (2016). Molecular hydrogen inhibits lipopolysaccharide-triggered NLRP3 inflammasome activation in macrophages by targeting the mitochondrial reactive oxygen species. *Biochimica et Biophysica Acta*, *1863*(1), 50–55.

Schuster, M., & Peter greenberg, E. P. (2006). A network of networks: Quorum-sensing gene regulation in *Pseudomonas aeruginosa*. *International Journal of Medical Microbiology: IJMM*, *296*(2-3), 73–81.

Schwarzer, C., Fu, Z., Morita, T., Whitt, A. G., Neely, A. M., Li, C., & Machen, T. E. (2015). Paraoxonase 2 serves a proapopotic function in mouse and human cells in response to the *Pseudomonas aeruginosa* quorum-sensing molecule N-(3-oxododecanoyl)-homoserine lactone. *The Journal of Biological Chemistry*, *290*(11), 7247–7258.

Schwarzer, C., Fu, Z., Patanwala, M., Hum, L., Lopez-Guzman, M., Illek, B., … Machen, T. E. (2012). *Pseudomonas aeruginosa* biofilm-associated homoserine lactone C12 rapidly activates apoptosis in airway epithelia. *Cellular Microbiology*, *14*(5), 698–709.

Shan, M., Gentile, M., Yeiser, J. R., Walland, A. C., Bornstein, V. U., Chen, K., … Cerutti, A. (2013). Mucus enhances gut homeostasis and oral tolerance by delivering immunoregulatory signals. *Science*, *342*(6157), 447–453.

Shi, J., Zhao, Y., Wang, K., Shi, X., Wang, Y., Huang, H., … Shao, F. (2015). Cleavage of GSDMD by inflammatory caspases determines pyroptotic cell death. *Nature*, *526*(7575), 660–665.

Shi, J., Zhao, Y., Wang, Y., Gao, W., Ding, J., Li, P., … Shao, F. (2014). Inflammatory caspases are innate immune receptors for intracellular LPS. *Nature*, *514*(7521), 187–192.

Shiner, E. K., Rumbaugh, K. P., & Williams, S. C. (2005). Inter-kingdom signaling: Deciphering the language of acyl homoserine lactones. *FEMS Microbiology Reviews*, *29*(5), 935–947.

Shirazi, T., Longman, R. J., Corfield, A. P., & Probert, C. S. (2000). Mucins and inflammatory bowel disease. *Postgraduate Medical Journal*, *76*(898), 473–478.

Van der Sluis, M., De Koning, B. A. E., De Bruijn, A. C. J. M., Velcich, A., Meijerink, J. P. P., Van Goudoever, J. B., … Einerhand, A. W. C. (2006). Muc2-deficient mice spontaneously develop colitis, indicating that MUC2 is critical for colonic protection. *Gastroenterology*, *131*(1), 117–129.

Smith, R. S., Fedyk, E. R., Springer, T. A., Mukaida, N., Iglewski, B. H., & Phipps, R. P. (2001). IL-8 production in human lung fibroblasts and epithelial cells activated by the *Pseudomonas* autoinducer N-3-oxododecanoyl homoserine lactone is transcriptionally regulated by NF-kappa B and activator protein-2. *Journal of Immunology*, *167*(1), 366–374.

Tao, S., Luo, Y., Bin he, He, Liu, J., Qian, X., Ni, Y., & Zhao, R. (2016). Paraoxonase 2 modulates a proapoptotic function in LS174T cells in response to quorum sensing molecule N-(3-oxododecanoyl)-L-homoserine lactone. *Scientific Reports*, *6*, 28778.

Valentine, C. D., Anderson, M. O., Papa, F. R., & Haggie, P. M. (2013). X-box binding protein 1 (XBP1s) is a critical determinant of *Pseudomonas aeruginosa* homoserine lactone-mediated apoptosis. *PLoS Pathogens*, *9*(8), e1003576.

Vikström, E., Bui, L., Konradsson, P., & Magnusson, K. E. (2009). The junctional integrity of epithelial cells is modulated by *Pseudomonas aeruginosa* quorum sensing molecule through phosphorylation-dependent mechanisms. *Experimental Cell Research*, *315*(2), 313–326.

Vikström, E., Bui, L., Konradsson, P., & Magnusson, K. E. (2010). Role of calcium signalling and phosphorylations in disruption of the epithelial junctions by *Pseudomonas aeruginosa* quorum sensing molecule. *European Journal of Cell Biology*, *89*(8), 584–597.

Vikström, E., Tafazoli, F., & Magnusson, K. E. (2006). *Pseudomonas aeruginosa* quorum sensing molecule N-(3 oxododecanoyl)-L-homoserine lactone disrupts epithelial barrier integrity of Caco-2 cells. *FEBS Letters*, *580*(30), 6921–6928.

Wickens, M., & Cox, M. M. (2009). Critical reviews in biochemistry and molecular biology. Introduction. *Critical Reviews in Biochemistry and Molecular Biology*, *44*(1), 2.

Wu, H., Li, X. M., Wang, J. R., Gan, W. J., Jiang, F. Q., Liu, Y., … Li, J. M. (2016). NUR77 exerts a protective effect against inflammatory bowel disease by negatively regulating the TRAF6/TLR-IL-1R signalling axis. *The Journal of Pathology*, *238*(3), 457–469.

Yue, C., Ma, B., Zhao, Y., Li, Q., & Li, J. (2012). Lipopolysaccharide-induced bacterial translocation is intestine site-specific and associates with intestinal mucosal inflammation. *Inflammation*, *35*(6), 1880–1888.

Zheng, L., Xu, Y., Lu, J., Liu, M., Bin, D., Miao, J., & Yin, Y. (2016). Variant innate immune responses of mammary epithelial cells to challenge by *Staphylococcus aureus*, *Escherichia coli* and the regulating effect of taurine on these bioprocesses. *Free Radical Biology & Medicine*, *96*, 166–180.

How to cite this article: Tao S, Sun Q, Cai L, et al. Caspase-1-dependent mechanism mediating the harmful impacts of the quorum-sensing molecule N-(3-oxo-dodecanoyl)-L-homoserine lactone on the intestinal cells. *J Cell Physiol*. 2018;1–13. https://doi.org/10.1002/jcp.27132